GLOBAL THREE-DIMENSIONAL MODELING STUDIES OF TROPOSPHERIC OZONE AND RELATED GASES

Final report to the NASA Atmospheric Chemistry Modeling and Analysis Program
(NASA Agreement No. NAG-1-1909)
Program Manager: P. DeCola
Performance period: 4/1/1997-3/31/2000

Investigators: M.B. McElroy (P.I.), D.J. Jacob (Co-P.I.), J.A. Logan (Co-I.), C.M. Spivakovsky (Co-I.)

1. ACCOMPLISHMENTS

We have used support from ACMAP over the past three years to conduct a range of activities as described below. A list of papers acknowledging support from ACMAP is attached.

1.1 Harvard-GISS2 Model Simulations of Tropospheric Ozone.

1.1.1 Model development and evaluation.

The Harvard-GISS2 global 3-D model uses a 4-hourly archive of meteorological data from the GISS GCM 2 [Hansen et al., 1983]. It has 4°x5° horizontal resolution and 9 vertical levels (7-8 in the troposphere). In its current implementation for tropospheric O_3-NO_x-HC chemistry the model includes ~100 interactive species and 24 tracers, and uses the fast Gear solver of Jacobson and Turco [1994] to integrate the chemical mechanism [Horowitz et al., 1998; Liang et al., 1998; Horowitz and Jacob, 1999; Jacob et al., 1999]. The model includes detailed emission and deposition algorithms coupled to the GCM meteorology [Wang et al., 1998a]. Cross-tropopause transport is specified as a monthly and latitudinally varying flux boundary condition at 150 hPa [Wang et al., 1998a] and amounts globally to 410 Tg O_3 yr^{-1}. We contributed results from this model to the AEAP and IPCC subsonic aviation assessments [Friedl et al, 1998; IPCC, 1999].

Global evaluation of the model with a detailed ensemble of surface, ozonesonde, and aircraft observations was presented by Wang et al. [1998b]. The model reproduces seasonal and latitudinal variations of tropospheric O_3 reasonably well [Logan, 1999]. The vertical gradient in the tropics is often too weak, apparently because the trade wind inversion is not strong enough. The model reproduces generally to within a factor of 2 the mean concentrations of NO and PAN observed in aircraft missions over different regions of the world, but tends to overestimate HNO_3 in the remote troposphere (sometimes several fold). Model concentrations of H_2O_2 are generally within a factor of 2 of observed values. A more focused evaluation of the model simulation of the polluted boundary layer was conducted by Horowitz et al. [1998] and Liang et al. [1998] using observed seasonal statistics for O_3 and related species at surface sites in North America. The largest discrepancy was a 15-20 ppbv overestimate of O_3 over the southeastern U.S. in summer which we traced to a Bermuda High anomaly in the GCM.

1.1.2 Global features of the O_3 budget.

We applied the Harvard-GISS2 model to investigate the factors controlling the global-scale distribution of tropospheric O_3 [Wang et al., 1998c]. We found that the budget of O_3 is dominated globally by chemical production and loss within the troposphere, and that these two terms are in close balance at all latitudes except the polar regions in winter. By tagging in the model O_3 produced in the stratosphere and in different regions in the troposphere, we found that the contribution of transport from the stratosphere to O_3 concentrations is about 30% at mid latitudes in winter, 10% in summer, and 5% in the tropics. The middle troposphere is a major global source region for O_3 even though it is not a region of net O_3 production. The observed O_3 spring maximum in the remote northern hemisphere is well reproduced by the model, where it is caused in part by transport from the stratosphere and in part by long-range transport of O_3 pollution (which is more efficient in spring than in summer because of the longer photochemical lifetime of O_3 in spring). Our results do not support previous explanations of the springtime maximum as due to wintertime accumulation of O_3 or its precursors in the Arctic.

1.1.3 North America: export and import of O_3 pollution.

We used the model to examine export of O_3 and NO_y species from the U.S. boundary layer to the global atmosphere [Horowitz et al., 1998; Liang et al., 1998], and to track the influence of fossil fuel combustion on NO_x in different regions of the northern hemisphere [Horowitz and Jacob, 1999] (work funded jointly by NSF). We found that 20% of the fossil fuel NO_x in the United States is exported from the boundary layer as NO_x or peroxyacylnitrates (PANs) (15% in summer, 25% in winter), primarily to the North Atlantic. The annual mean export of NO_x and PANs from the U.S. boundary layer was estimated to be 1.2 Tg N yr^{-1}, representing an important source of NO_x on the scale of the northern hemisphere. By tagging fossil fuel NO_x and its reservoir NO_y species [Horowitz and Jacob, 1999], we found that fossil fuel combustion accounts for over 40% of NO_x concentrations in the lower and middle troposphere throughout the extratropical northern hemisphere in summer. Long-range transport as PANs is responsible for over 80% of the fossil fuel NO_x in the lower troposphere over the oceans. We found that the U.S. contribute about half of the fossil fuel NO_x over the North Atlantic in summer, while China contributes about half of the fossil fuel NO_x over the western North Pacific.

We also applied the model to examine the effect of rapid industrialization in eastern Asia on surface O_3 air pollution in the United States [Jacob et al., 1999] (work funded jointly by EPRI). We found that the tripling of Asian NO_x emissions expected from 1985 to 2010 [van Aardenne et al., 1999] should increase monthly mean O_3 concentrations by 2-6 ppbv in the western United States and by 1-3 ppbv in the eastern United States, with maximum effect in April-June. This increase would more than offset the benefits of 25% domestic reductions in anthropogenic emissions of NO_x and HC in the western United States. We noted that Asian influence would probably be less under the stagnant conditions leading to violations of the U.S. air quality standard.

1.1.4 Long-term trends in tropospheric O_3.

In another application of the Harvard-GISS2 model, we investigated the changes in tropospheric O_3 and OH since 1850 caused by increases in fossil fuel combustion and industry, biomass burning, and CH_4 [Wang and Jacob, 1998]. Our model results indicate a 63% increase in the tropospheric O_3 inventory (NH, 80%; SH, 50%) which closely parallels the rise in CO and HC emissions, because the O_3 yield per mole of CO or HC oxidized has remained nearly constant. In contrast, the O_3 production efficiency per mole of NO_x emitted has decreased globally by a factor of 2. We find little change (9% decrease) in global mean OH since 1850, reflecting compensating influences. Comparisons of model results with late 1800s O_3 data indicates a systematic overestimate of ~5 ppbv; correcting this requires either a large missing chemical sink for O_3 or a downward revision of natural NO_x sources. We are presently investigating this issue.

Calibration problems with the older data cannot be excluded [Pavelin et al., 1999].

1.1.5 Analysis of Trends in the Vertical Distribution of O_3.

We participated in the SPARC Ozone Trends Assessment [WMO, 1998; Randel et al., 1999], leading the analysis of ozonesonde data [Logan et al., 1999]. Trends in the sonde data were also computed by G. Tiao (U. Chicago) and colleagues. We derived similar trends to Tiao's group, and found that the major reason for different results was in data selection criteria, rather that in the statistical trend models. Tiao's group omitted more of the sonde data than we did in an effort to improve data quality; this did not necessarily lead to better defined trends because of the resulting increase in the variances of the monthly mean time series.

We find significant decreases in stratospheric O_3 at all stations in mid and high latitudes of the northern hemisphere for 1970-1996, with the largest decreases located at 12-21 km, and trends of -3 to -10 %/decade near 17 km. The mean midlatitude trend is largest, -7 %/decade, from 12 to 17.5 km for 1970-96. For 1980-96, the decrease is more negative by 1-2.5 %/decade, with a maximum trend of -10%/decade in the lowermost stratosphere. The trends vary seasonally from about 12 to 17.5 km, with largest O_3 decreases in winter and spring. Decreases in O_3 in the lower stratosphere are in excellent agreement with those derived from SAGE data [Cunnold et al., 1999].

Trends in tropospheric O_3 are highly variable and depend on region. At the 4 Canadian stations there are decreases or zero trends for 1970-96, and decreases of -2 to -8 %/decade in the mid-troposphere for 1980-96. The 3 European stations show increases of 5-25% for 1970-96, but trends are close to zero for two stations for 1980-96 and positive for one; most of the increase was before 1985. There are increases in O_3 for the 3 Japanese stations for 1970-96 of 10-15%, decreasing with increasing altitude, but trends are either positive or zero for 1980-96; the U.S. stations show zero or slightly negative trends in tropospheric O_3 after 1980.

We have used the Harvard-GISS2 model to investigate the causes of trends in tropospheric O_3 since 1970. We developed emission estimates for 1970 for anthropogenic NO_x, CO, and HC by using available inventory data for North America and Europe, and by scaling the 1985 inventory to fossil fuel use for other countries. We find that increasing anthropogenic emissions over Europe may have produced O_3 increases of 2-4%/decade from 1970 to 1985, while more rapid increases in Asian emissions appear to cause an O_3 increase of 3-5 %/decade; however, increasing emissions also causes O_3 to increase by 2-4 %/decade over Canada, contrary to observations. Accounting in the model for the decreases in the stratospheric O_3 column since 1970 (as observed from TOMS) yields decreases in tropospheric O_3 of only 0.2-1.0%/decade at northern midlatitudes. A 50% reduction of the stratospheric flux causes a decrease in midlatitude O_3 from 8% near the surface to 35% in the upper troposphere in winter (2-15% in summer); the observed trends are more uniform with altitude [Logan et al., 1999]. Perturbations to O_3 in the model at northern midlatitudes are generally well mixed in the midtroposphere, in contrast to the spatial patterns evident in the observed trends. There may be too rapid vertical or zonal mixing in the GISS2 model.

1.2 Development of GEOS-CHEM Model for Tropospheric O_3 Applications.

1.2.1 General development.

The GEOS-CHEM model uses the same (continually updated) emission, chemistry, and deposition modules as the Harvard-GISS2 model but is driven by the GEOS assimilated meteorological observations and a chemical tracer model (CTM) developed at the NASA/GSFC

DAO [Lin and Rood, 1996; Allen et al., 1996ab, with updates]. The GEOS data are available as a continuous archive starting in 1983 with temporal resolution of 3 to 6 h depending on the variable, and horizontal resolution of 2°x2.5°. The data up to 1995 (GEOS-1) have 20 vertical levels extending up to 10 hPa; subsequent data until 1998 (GEOS-STRAT) have 46 levels to better resolve the stratosphere; and the most recent data for 1998 to present (GEOS-2) have 70 levels. In our applications we use either the original 2°x2.5° resolution or a 4°x5° resolution with regridded GEOS fields for computational expediency; we also merge the stratospheric levels above 70 hPa. Anthropogenic emissions for simulation of specific years are adjusted from our base emission inventory for 1985 on a country-by-country basis, using national emission estimates for North America [EPA, 1999] and Europe [EMEP reports], and scaling to trends in fossil fuel use [Marland et al., 1999] for countries with no emission control policies.

We are developing the GEOS-CHEM model as a flexible tool for simulation of a wide range of issues in tropospheric chemistry, complementing base support from ACMAP with supplements from other sources. We elaborate below on projects supported specifically by NAG-1-1909. Other recent or ongoing projects include:

- Simulation of O_3 pollution over the United States (jointly supported by EPRI) to understand the contribution of long-range transport from anthropogenic sources outside North America. For this project we are carrying out a detailed analysis of the ability of the model to simulate chemical processes in the U.S. boundary layer, using data from the SOS and NARSTO-Northeast campaigns in the eastern United States in summer 1995. A preliminary comparison of model results with O_3 observations from the AIRS network in June 1995 is shown in Figure 1. Note that O_3 over the southeastern U.S. is well simulated, in contrast to the Harvard-GISS2 model where a Bermuda High anomaly caused a large overestimate.
- Simulation of $^{210}Pb/^{7}Be$ (jointly supported by NASA/SASS) to design and test a wet scavenging algorithm for soluble tracers. In addition to scavenging by large-scale and convective precipitation, we have implemented a revised version of the cirrus precipitation scheme of Lawrence and Crutzen [1998]. We find that entraining wet convection in the GEOS convective transport scheme allows the model to capture the observed ^{7}Be minimum in the tropics, unlike previous models [Brost et al., 1991; Koch et al., 1996] where ^{7}Be could descend in the tropical troposphere without experiencing scavenging. A preliminary account of our work was presented at the spring 1999 AGU meeting [Liu et al., 1999a].
- Development of CH_3I as a tracer of marine convection in global 3-D models (jointly supported by NSF) to complement ^{222}Rn which tests continental convection. Our preliminary results suggest that entrainment during GEOS deep marine convection events is insufficient, as reflected by a more pronounced C-shape in the simulated vertical profiles of CH_3I than in the observations. Our work also revealed major inconsistencies between different observational data sets for CH_3I in air and seawater, which we are now trying to resolve to arrive at a first credible global budget of atmospheric CH_3I. This work was presented at AGU meetings [Schultz et al., 1998; Hsu et al., 1999].
- Simulation of HCN (jointly supported by NSF) to explain the large seasonal variations seen in column observations [e.g., Rinsland et al., 1999] and to investigate the use of HCN as a biomass burning tracer detectable from space. We found that the available HCN observations could be consistent with a scenario where biomass burning provides the main source and ocean uptake provides the main sink. The resulting atmospheric lifetime of HCN would be 2 months, instead of 2 years due to reaction with OH as had been thought [Cicerone and Zellner, 1983]. This work is now published [Li et al., 2000].

as illustrated in Figure 4 by a comparison of model results to observed vertical profiles of O_3, CO, and PAN for PEM-West B flights 17 (35°-45°N) and 8 (15°-25°N). Strong continental outflow in flight 17 is reflected by the high concentrations of CO and PAN in the lower troposphere. The model captures the general features of the outflow although it cannot capture observed thin layers of very high CO, and it overestimates PAN in the upper troposphere. Ozone concentrations are not significantly elevated in the outflow, either in the model or in the observations, due to the weak photochemical activity in early spring at midlatitudes. The model tends to overestimate O_3 concentrations for the PEM-West B conditions, possibly because of inadequate accounting of heterogeneous losses of NO_x and O_3 in the aerosol-rich Asian plume [Dentener et al., 1996; Zhang et al., 1999].

1.2.4 Interannual variability of CO.

We have developed a capability for applying the GEOS-CHEM model to analyze interannual variability and trends of CO over the past decade [Novelli et al., 1998]. Our work goes beyond the early GEOS CTM study of Allen et al. [1996b] by accounting for CO-OH chemical coupling, interannual variability of emissions, and decreases in stratospheric O_3 column. Our first step has been to develop an improved polynomial parameterization for rapid computation of OH concentrations in the model [Duncan et al., 2000]. This parameterization has now been implemented in the GEOS-CHEM model and is being tested with single-year simulations.

The new OH parameterization, described by Duncan et al. [2000], improves on the original [Spivakovsky et al., 1990] by including NMHC chemistry (such as for isoprene) and using updated photochemical rate constants. It has been automated to facilitate the construction of parameterization functions using lower-order polynomials (for higher speed) and the achievement of a desired accuracy. The original parameterization program took as input an ensemble of photochemical model results spanning the range of independent variables and returned computer-generated FORTRAN functions as well as estimates of the accuracy of the approximation; if the accuracy achieved was insufficient, domains were divided into rectangular subdomains manually, and the parameterization procedure was repeated. In collaboration with M. Ko and D. Portman at AER, we upgraded the program to search automatically for the best subdivisions in the multidimensional domain; in addition, we interfaced the photochemical model calculations to the parameterization program to generate additional points as needed.

2. CONTRIBUTION TO EDUCATION.

Funds from this ACMAP grant have provided partial support for six Harvard graduate students and three Harvard postdocs:

- Yuhang Wang (Ph.D. 1998), now Assistant Professor in the Dept. of Environmental Sciences at Rutgers University;
- Larry W. Horowitz (Ph.D. 1998), now Visiting Scientist at NOAA/GFDL;
- Jinyou Liang (Ph.D. 1998), now Scientist at the California Air Resources Board;
- Hongyu Liu (G3)
- Arlene M. Fiore (G2)
- Qinbin Li (G2)
- Isabelle Bey (postdoc)
- Bryan N. Duncan (postdoc)
- Andrew C. Fusco (postdoc)

3. PUBLICATIONS ACKNOWLEDGING SUPPORT FROM NAG-1-1909

Cunnold, D. M., H. J. Wang, L. Thomason, J. Zawodny, J. A. Logan, and I. A. Megretskaia, SAGE (v.5.96) ozone trends in the lower stratosphere, *J. Geophys. Res.*, *105*, 4445-4457, 2000.

Duncan,, B., D. Portman, I. Bey and C. Spivakovsky: Parameterization of OH for efficient computation in chemical tracer models, *J. Geophys. Res.*, *105*, 12,259-12,262, 2000.

Horowitz, L.W., J. Liang, G.M. Gardner, and D.J. Jacob, Export of reactive nitrogen from North America during summertime, *J. Geophys. Res. 103*, 13451-13476, 1998.

Horowitz, L. W., and D. J. Jacob, Global impact of fossil fuel combustion on atmospheric NO$_x$, *J. Geophys. Res.*, *104*, 23823-23840, 1999.

Jacob, D. J., J. A. Logan, and P. P. Murti, Effect of rising Asian emissions on surface ozone in the United States, *Geophys. Res. Lett.26*, 2175-2178, 1999.

Li, Q., D. J. Jacob, I. Bey, R. M. Yantosca, Y. Zhao, and Y. Kondo, Atmospheric Hydrogen Cyanide (HCN): Biomass Burning Source, Ocean Sink?, *Geophys. Res. Lett.*, *27*, 357-360, 2000.

Liang, J., L. W. Horowitz, D. J. Jacob, Y. Wang, A. M. Fiore, J. A. Logan, G. M. Gardner, and J. W. Munger, Seasonal budgets of reactive nitrogen species and ozone over the United States, and export fluxes to the global atmosphere, *J. Geophys. Res.*, *103*, 13,435-13,450, 1998.

Logan, J. A., I. A. Megretskaia, A. J. Miller, G. C. Tiao, et al. Trends in the vertical distribution of ozone: a comparison of two analyses of ozonesonde data, *J. Geophys. Res.*, *104*, 26373-26399, 1999.

Randel, W., R. Stolarski, D. Cunnold, J. A. Logan, and M. J. Newchurch, Trends in the vertical distribution of ozone, *Science,285*, 1689-1692, 1999.

Singh, H., Y. Chen, L. Salas, D. Herlth, R. Kolyer, A. Tabazadeh, Y. Fukui, I. Bey, R. Yantosca, D. J. Jacob, et al. Distributon and fate of select oxygenated organic species in the troposphere and lower stratosphere over the Atlantic, *J. Geophys. Res.*, *105*, 3795-3806, 2000.

Spivakovsky, C. M., J. A. Logan, S. A. Montska, Y. J. Balkanski, M. Foremen-Fowler, D. B. A. Jones, L. W. Horowitz, A. C. Fusco, C. A. M. Brenninkmeijer, M. J. Prather, S. C. Wofsy, and M. B. McElroy, Three dimensional climatological distribution of tropospheric OH: update and evaluation, *J. Geophys. Res.*, *105*, 8931-8980, 2000.

Wang, Y. H., D. J. Jacob, and J. A. Logan, Global simulation of tropospheric O$_3$-NO$_x$-Hydrocarbon chemistry, 1. Model formulation, *J. Geophys. Res. 103*, 10,713-10,726, 1998.

Wang, Y. H., J. A. Logan, and D. J. Jacob, Global simulation of tropospheric O$_3$-NO$_x$-Hydrocarbon chemistry, 2. Model evaluation, *J. Geophys. Res. 103*, 10,727-10,756, 1998.

Wang, Y. H., D. J. Jacob, and J. A. Logan, Global simulation of tropospheric O$_3$-NO$_x$-Hydrocarbon chemistry, 3. Origin of tropospheric ozone and effects of non-methane hydrocarbons, *J. Geophys. Res. 103*, 10,757-10,768, 1998.

Wang, Y. H. and D. J. Jacob, Anthropogenic forcing on tropospheric ozone and OH since preindustrial times, *J. Geophys. Res.*, *103*, 31123-31135, 1998.

4. REFERENCES.

Allen, D. J., R. B. Rood, A. M. Thompson, and R. D. Hudson, Three dimensional radon 222

Sillman, and M.J. Prather, Factors regulating ozone over the United States and its export to the global atmosphere, *J. Geophys. Res.*, *98*, 14,817-14,826, 1993.

Jacob, D. J., J. A. Logan, and P. P. Murti, Effect of rising Asian emissions on surface ozone in the United States, *Geophys. Res. Lett.*, *26*, 2175-2178, 1999.

Jacobson, M.Z., and R.P. Turco, SMVGEAR: a sparse-matrix, vectorized Gear code for atmospheric models, *Atmos. Environ.*, *28*, 273-284, 1994.

Koch, D. M., D. J. Jacob, and W. C. Graustein, Vertical transport of tropospheric aerosols as indicated by ^{7}Be and ^{210}Pb in a chemical tracer model, *J. Geophys. Res.*, *101*, 18,651-18,666, 1996.

Lawrence, M.G., and P. J. Crutzen, The impact of cloud particle gravitational settling on soluble trace gas distributions. *Tellus, B50*, 263-289, 1998.

Li, Q., D. J. Jacob, I. Bey, R. M. Yantosca, Y. Zhao, and Y. Kondo, Atmospheric Hydrogen Cyanide (HCN): Biomass Burning Source, Ocean Sink?, *Geophys. Res. Lett.*, *27*, 357-360, 2000.

Liang,J., L. W. Horowitz, D. J. Jacob, Y. Wang, A. M. Fiore, J. A. Logan, G. M. Gardner, and J. W. Munger, Seasonal budgets of reactive nitrogen species and ozone over the United States, and export fluxes to the global atmosphere, *J. Geophys. Res.*, *103*, 13,435-13,450, 1998.

Lin, S.-J., and R.B. Rood, Multidimensional flux-form semi-Lagrangian transport schemes, *Mon. Weather Rev.*, *124*, 2046-2070, 1996.

Liu, H. Y., D. J. Jacob, I. Bey, R. M. Yantosca, and D. M. Koch, Three-dimensional simulation of ^{210}Pb and ^{7}Be in the Harvard-DAO tropospheric chemistry model, *Eos Trans. AGU, 80 (17)*, S32, 1999a.

Logan, J.A., Trends in the vertical distribution of ozone: An analysis of ozonesonde data, *J. Geophys. Res.*, *99*, 25553-25585, 1994.

Logan, J. A., An analysis of ozonesonde data for the troposphere: Recommendations for testing 3-D models, and development of a gridded climatology for tropospheric ozone, *J. Geophys. Res. 104*, 16,115-16,149, 1999.

Logan, J. A., I. A. Megretskaia, A. J. Miller, G. C. Tiao, et al. Trends in the vertical distribution of ozone: a comparison of two analyses of ozonesonde data, *J. Geophys. Res.*, *104*, 26373-26399, 1999.

Marland, G., T. A. Boden, R. J. Andres, A. L. Brenkert, and C. A. Johnston, Global, Regional, and National Fossil Fuel CO_2 Emissions, Trends Online: A Compendium of Data on Global Change. Oak Ridge National Laboratory, U.S. Department of Energy, Oak Ridge, Tennessee, http://cdiac.ESD.ORNL.GOV/trends/emis/em_cont.htm, 1999.

McLinden, C., S. Olsen, B. Hannegan, O. Wild, and M. Prather, Stratospheric ozone in 3D models: a simple chemistry and the cross-tropopause flux, submitted to *J. Geophys. Res.*, 2000.

Murphy, D.M., D.W. Fahey, M.H. Proffitt, S.C. Lui, K.R. Chang, C.S. Eubank, S.R. Kawa, and K.K. Kelly, Reactive nitrogen and its correlation with ozone in the lower stratosphere and upper troposphere, *J. Geophys. Res.*, *98*, 8751-8775, 1993.

Novelli, P. C., K. A. Masarie and P. M. Lang, Distributions and recent changes of carbon monoxide in the lower troposphere, *J. Geophys. Res.*, *103*, 19,015-19,033, 1998.

Pavelin, E.G., C. E. Johnson, S. Rughooputh, and R. Toumi, Evaluation of pre-industrial surface ozone measurements made using Schonbein's method. *Atmos. Environ.*, *33*, 919-929, 1999.

5929-5941, 1997.

Randel, W. J., R. S. Stolarski, D. M. Cunnold, J. A. Logan, M. J. Newchurch, and J. Zawodny, Trends in the vertical distribution of ozone, *Science, 285*, 1689-1692, 1999.

Schubert, S.D., R.B. Rood, and J. Pfaendtner, An assimilated data set for Earth Science applications, *Bull. Am. Met. Soc., 74,* 2331-2342, 1993.

Schultz, M. G., L. Hsu, D. J. Jacob, T. Chen, and D. R. Blake, Using methyl iodide as a tracer for marine convection in a global 3-dimensional model, *Eos Trans. AGU, 79 (45)*, F116, 1998.

Singh, H., Y. Chen, L. Salas, D. Herlth, R. Kolyer, A. Tabazadeh, Y. Fukui, I. Bey, R. Yantosca, D. J. Jacob, et al. Distributon and fate of select oxygenated organic species in the troposphere and lower stratosphere over the Atlantic, *J. Geophys. Res., 105*, 3795-3806, 2000.

Spivakovsky, C. M., J. A. Logan, S. A. Montska, Y. J. Balkanski, M. Foremen-Fowler, D. B. A. Jones, L. W. Horowitz, A. C. Fusco, C. A. M. Brenninkmeijer, M. J. Prather, S. C. Wofsy, and M. B. McElroy, Three dimensional climatological distribution of tropospheric OH: update and evaluation, *J. Geophys. Res., 105*, 8931-8980, 2000.

Van Aardenne, J. A., G. R. Carmichael, H. Levy II, D. Streets, and L. Hordijk, Anthropogenic NO_x emissions in Asia in the period 1990-2020, *Atmos. Environ., 33*, 633-646, 1999.

Wang, Y. H., D. J. Jacob, and J. A. Logan, Global simulation of tropospheric O_3-NO_x-Hydrocarbon chemistry, 1. Model formulation, *J. Geophys. Res. 103*, 10,713-10,726, 1998.

Wang, Y. H., J. A. Logan, and D. J. Jacob, Global simulation of tropospheric O_3-NO_x-Hydrocarbon chemistry, 2. Model evaluation, *J. Geophys. Res. 103*, 10,727-10,756, 1998.

Wang, Y. H., D. J. Jacob, and J. A. Logan, Global simulation of tropospheric O_3-NO_x-Hydrocarbon chemistry, 3. Origin of tropospheric ozone and effects of non-methane hydrocarbons, *J. Geophys. Res. 103*, 10,757-10,768, 1998.

Wang, Y. H. and D. J. Jacob, Anthropogenic forcing on tropospheric ozone and OH since preindustrial times, *J. Geophys. Res., 103*, 31123-31135, 1998.

WMO, World Meteorological Organization, Assessment of trends in the vertical distribution of ozone, SPARC Report no. 1, Global Ozone Res. Monit. Proj., *WMO, Rep. 43*, Geneva, 1998.

Zhang, Y., and G.R. Carmichael, The role of mineral aerosol in tropospheric chemistry in East Asia - A model study, *J. Appl. Met., 38*, 353-366, 1999.

Figure Captions.

Figure 1. Mean afternoon (1-4 pm) ozone concentrations in surface air over the United States in June 1995. Top panel: Harvard GEOS results. Middle panel: Observations form the AIRS network. Bottom panel: simulated verses observed ozone for individual 2°x2.5° model grid squares over the U.S. The solid line shows a 1:1 relationship.

Figure 2. Comparison of Harvard-GEOS model results (filled circles) to observed monthly mean CO concentrations at surface sites (solid lines and open triangles) [Novelli et al., 1998].

Figure 3. Comparison of Harvard-GEOS model results (dashed lines) to observed vertical profiles of ozone (solid lines) for January, March, July and October. The solid bars represent the standard deviations of the observations [Logan, 1999].

Figure 4. Comparison of Harvard-GEOS model results to vertical profiles of O_3, CO, and PAN observed during PEM-West B flights 17 and 8. Flight 17 (2/17/94) took place over the Sea of Japan between 35° and 45°N while flight 8 (3/11/94) took place further south between 15° and 25°N. Observed concentrations are shown as symbols; the colored lines are model results for the day of the flight and for the different gridboxes covered by the flight track.

Fig. 1

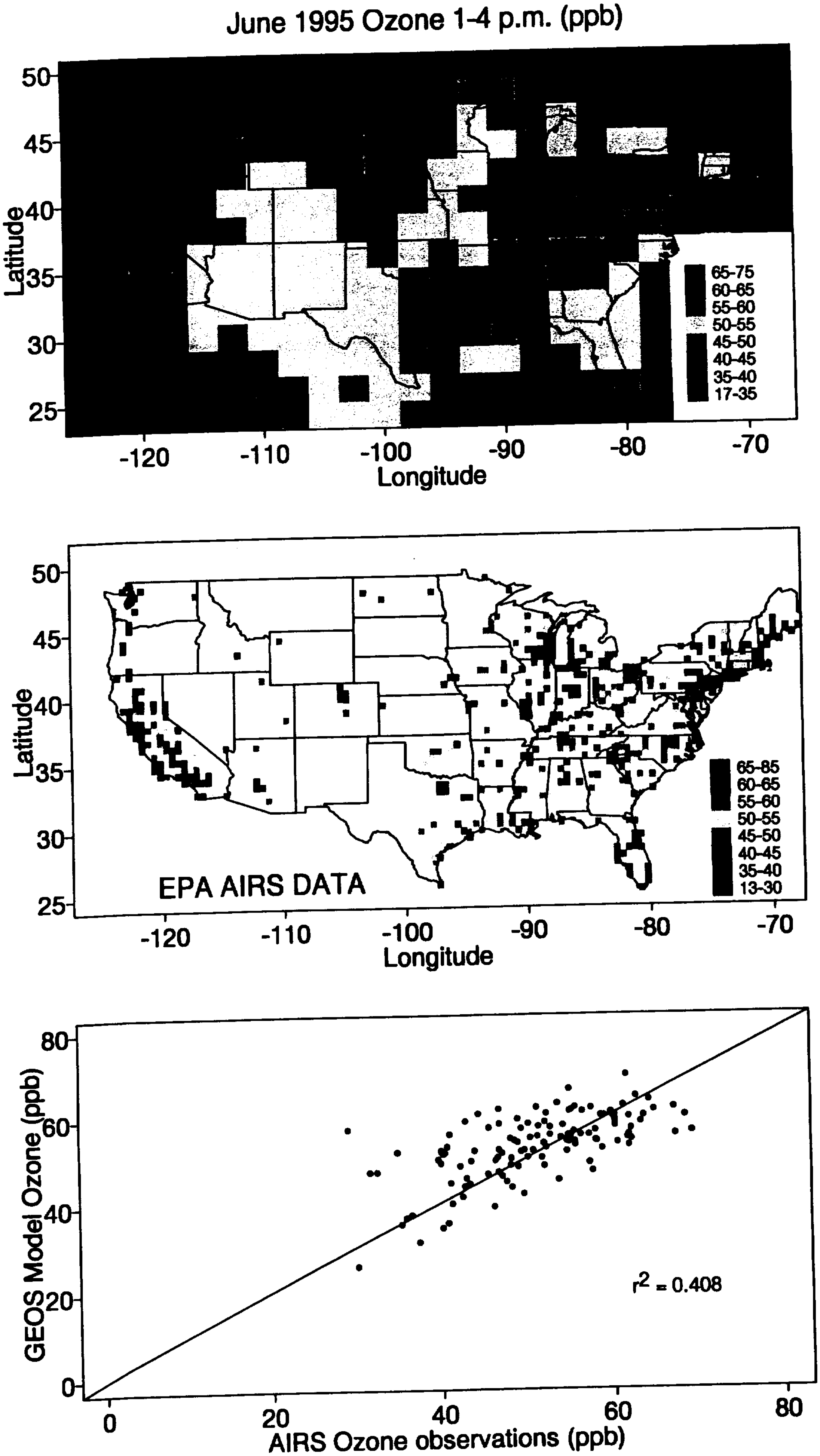

June 1995 Ozone 1-4 p.m. (ppb)
Latitude
50
45
40
35
30
25
-120
-110
-100
-90
-80
-70
Longitude
65-75
60-65
55-60
50-55
45-50
40-45
35-40
17-35
Latitude
50
45
40
35
30
25
EPA AIRS DATA
65-85
60-65
55-60
50-55
45-50
40-45
35-40
13-30
-120
-110
-100
-90
-80
-70
Longitude
GEOS Model Ozone (ppb)
80
60
40
20
0
$r^2 = 0.408$
0
20
40
60
80
AIRS Ozone observations (ppb)

Figure 2.

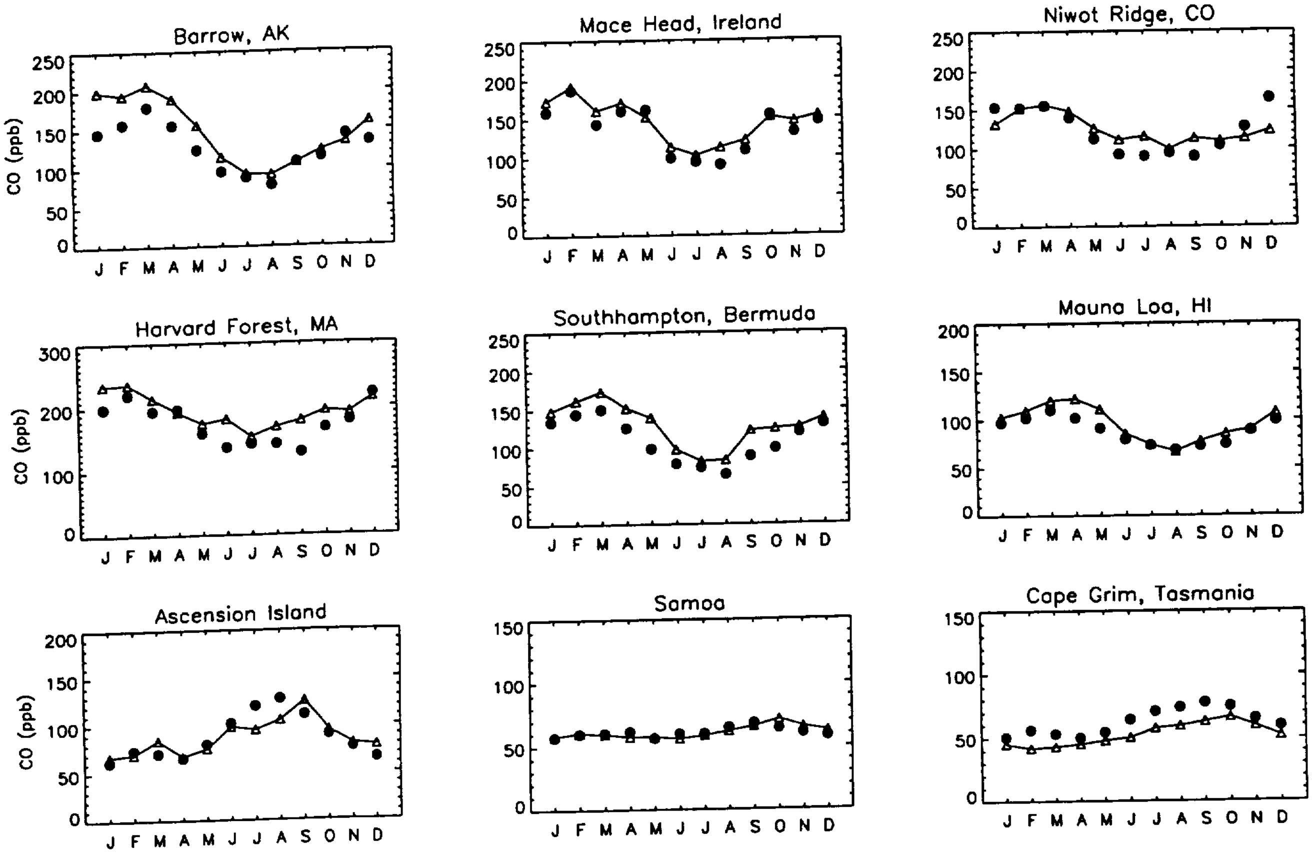
Barrow, AK
Mace Head, Ireland
Niwot Ridge, CO
Harvard Forest, MA
Southhampton, Bermuda
Mauna Loa, HI
Ascension Island
Samoa
Cape Grim, Tasmania
CO (ppb)
0
50
100
150
200
250
300
J F M A M J J A S O N D

Figure 3

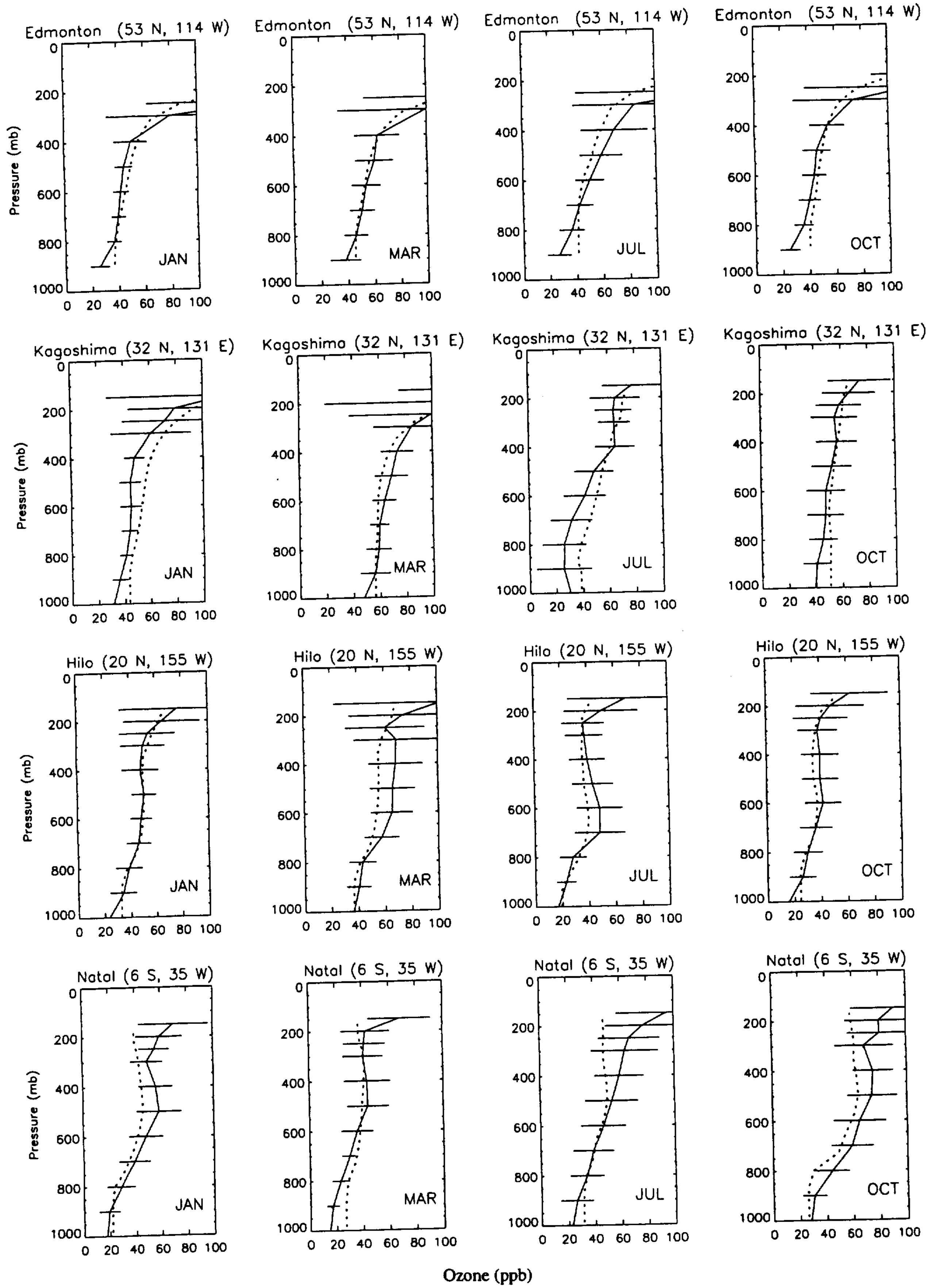
Edmonton (53 N, 114 W)
JAN
MAR
JUL
OCT
Kagoshima (32 N, 131 E)
JAN
MAR
JUL
OCT
Hilo (20 N, 155 W)
JAN
MAR
JUL
OCT
Natal (6 S, 35 W)
JAN
MAR
JUL
OCT
Pressure (mb)
0
200
400
600
800
1000
0
20
40
60
80
100
Ozone (ppb)

Figure 3 (cont)

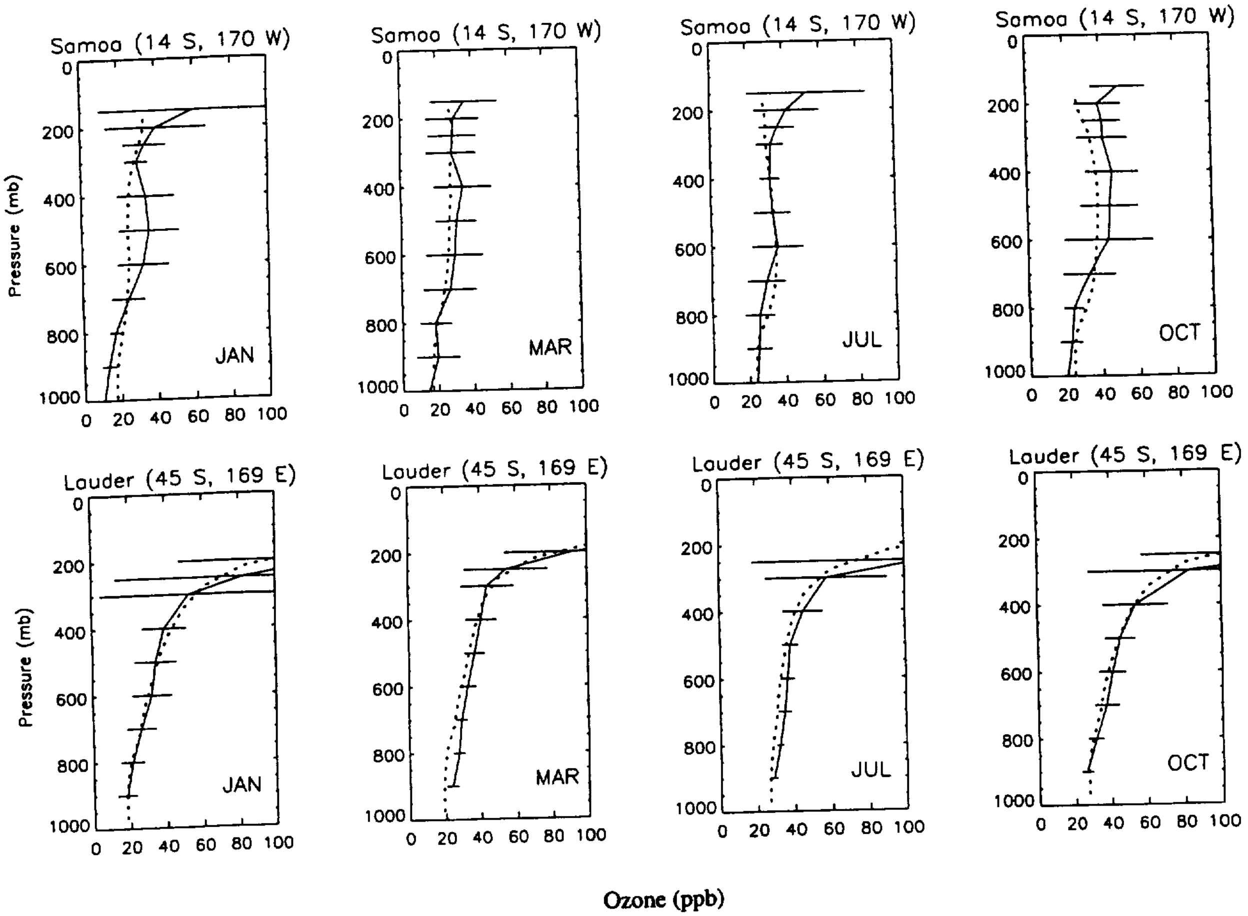

Comparison between modeled and observed concentrations during flights 17 and 8

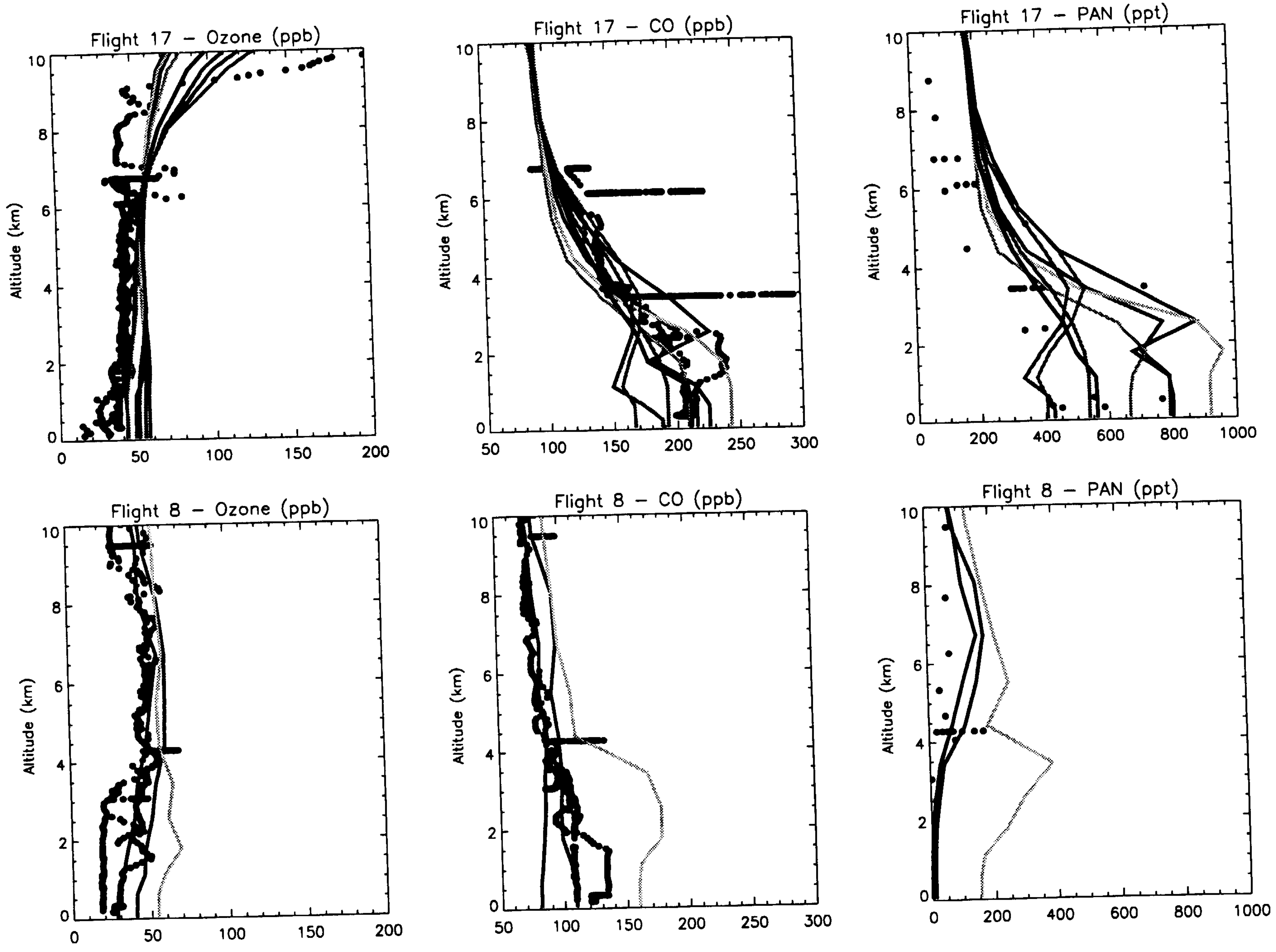

Fig. 4